Available online at www.sciencedirect.com
ScienceDirect
Trans. Nonferrous Met. Soc. China 27(2017) 467−474
Transactions of Nonferrous Metals Society of China
www.tnmsc.cn

Effects of melt viscosity on enrichment and separation of primary silicon from Al−Si melt

Wen-zhou YU[1], Wen-hui MA[2], Zhong ZHENG[1], Wei-yan JIANG[1], Jie LI[1], Mao-hong TIAN[1]

1. College of Materials Science and Engineering, Chongqing University, Chongqing 400044, China;
2. Faculty of Metallurgical and Energy Engineering,
Kunming University of Science and Technology, Kunming 650093, China

Received 7 December 2015; accepted 28 November 2016

Abstract: The effects of melt viscosity on the enrichment and separation of Si crystals from Al–Si melt during an electromagnetic solidification process were investigated. Both the enrichment efficiency and the separation were found to be strongly dependent on the melt viscosity. A high melt viscosity was beneficial to the enrichment of primary silicon, whereas a low melt viscosity facilitated the separation process. A new enrichment mechanism was proposed in order to clarify the influence of melt viscosity, and an improved process for achieving high-efficiency enrichment of Si crystals via control of the melt viscosity was also proposed. Additionally, the morphology of Si crystals was found to change from spheroidal to plate-like in shape owing to the difference in viscosities in different regions.

Key words: directional solidification; electromagnetic stirring; Al−Si melt; primary silicon; separation; viscosity

1 Introduction

Exploitation of solar energy is attracting increasing attention as a solution to problems of environmental pollution and shortage of conventional (fossil) energy sources. Conventionally, solar cells are dependent on expensive semiconductor-grade silicon (SEG-Si, 99.9999999% purity), which is manufactured by the Siemens process. With the aims of producing solar-grade silicon (SOG-Si, 99.9999% purity), a modified Siemens process and a fluidized bed reactor process have recently been developed. However, the potential for cost reduction in these processes is limited because the Si productivity is low [1]. A metallurgical route, which usually includes acid leaching [2], oxidation treatment [3], vacuum melting [4], slag refining [5], directional solidification [6,7], and electron beam melting [8], has been proposed to deal with the metallurgical grade silicon (MG-Si, 98%−99.9% purity) by removing the impurities from it for the demand of SOG-Si, and it is considered as a potential method for achieving cost reduction.

In recent years, considerable progress has been made toward reducing cost further by alloying Si with other elements such as Al [9], Sn [10], Cu [11], and Fe [12]. This method has the following outstanding advantages: 1) the refining temperature is much lower than the melting temperature of Si (i.e., 1687 K), 2) the solid/liquid segregation of impurities is enhanced at low temperatures, and 3) the process is environmentally friendly.

Al−Si alloy refining [13−15] is a highly promising process for low-cost SOG-Si production and is one of the few MG-Si purification processes which is realized on the industrial scale [16]; thus, this alloy system at low temperature has received extensive research attention. Generally, Si purification using Al−Si alloy is performed in three steps: 1) fusing the mixture of MG-Si and metal Al to obtain a hypereutectic Al−Si melt, 2) cooling the melt slowly to induce nucleation and growth of primary Si, and 3) acid leaching to remove Al and other impurities for collecting Si crystals. However, considerable amounts of aluminum and silicon are wasted during the process of acid leaching. Therefore, efficient enrichment and separation of Si crystals before

Foundation item: Project (u1137601) supported by the National Natural Science Foundation of China; Project (106112015CDJXY130007) supported by Fundamental Research Funds for the Central Universities, China
Corresponding author: Wen-zhou YU; Tel: + 86-23-65102011; E-mail: yuwenzhoucd@cqu.edu.cn
DOI: 10.1016/S1003-6326(17)60053-0

acid leaching are crucial for achieving cost reduction and environmental conservation. Electromagnetic separation is an effective method for promoting the migration of Si crystals in order to improve their enrichment efficiency during the solidification of Al−Si alloy [17−21]. Melt viscosity is a key factor influencing the movement of Si crystals in Al–Si melt during the electromagnetic separation process [22]. However, no study has thus far been focused on the mechanism of influence of melt viscosity on the enrichment and separation of Si. The influence of melt viscosity needs to be investigated thoroughly in order to improve the enrichment efficiency of Si in Al−Si melt.

In the present work, the influence of melt viscosity on the enrichment of Si crystals is examined and a new Si enrichment mechanism is proposed in order to clarify the influence of melt viscosity. The influence of melt viscosity on the separation process is also analyzed.

2 Experimental

Hypereutectic Al−Si alloys were prepared by mixing of metallurgical-grade Si (99.9%) powder and pure Al (99.99%) powder in a graphite crucible and subsequently melting the mixture to obtain alloys in an electrical resistance-heating furnace. Finally, through adjustment of the mass fractions of Si and Al, Al−25% Si, Al−35%Si, and Al−45% Si alloys were prepared. The total mass of each sample was 80 g. The process of silicon enrichment was performed by placing samples of the prepared alloys at the center of the coil zone of a 60 kW high-frequency induction furnace and then heating the samples until they were melted completely. After the samples had been melted, they were pulled down by a pulling system. The pulling rate was controlled at 7 μm/s, and the temperature gradient was 35−40 K/cm in the axial direction of the sample. For specific experiments, the pulling distance was set to 6 cm, 8 cm, and 10 cm in the downward direction from the lower end of the induction coil. During the pulling-down process, the current intensity was controlled at 12 A. After completion of the enrichment, separation of the enriched Si crystals from the Al−Si melt was performed by removing the graphite crucible from the induction furnace and then dumping the crucible to pour out the Al−Si melt rapidly. A schematic diagram of the experimental setup is shown in Fig. 1.

After solidification, the alloy samples were cut in the longitudinal direction to examine the enrichment of primary silicon crystals. The surface of the samples was ground with SiC paper for metallographic observations. The macrostructures and microstructures of the solidified samples were observed with a SONY digital camera and Olympus PME3 light optical microscope (LOM) with an attached KAPPA image analyzer, respectively. The Si enrichment region was cut out from the sample and then subjected to atomic absorption spectroscopy (AAS) measurement for observing the Si content. X-ray diffraction (XRD, Advance D8) was used to characterize the preferential growth face of primary silicon in the enrichment zone. For the XRD characterization, the enrichment zone in different positions was cut down from the sample and polished. The XRD pattern from 20° to 120° was used to confirm the preferred growth orientation with a Cu K_α radiation resource. The viscosity of semisolid Al−Si melt was measured using a high-temperature viscometer (self-designed by Kunming University of Science and Technology), which consisted of an outer cylinder (crucible) and an inner cylinder. Both cylinders were made of graphite. The shear rate was controlled at 10 s^{-1} by adjusting the angular rotation speed of the motor. During the measurement, the samples were kept inside an argon-recirculating furnace to maintain the apparatus in an isothermal condition (±1 °C). The viscosity measurement experiment was repeated three to five times at a given temperature, and the mean values were taken as the apparent viscosities of the melts.

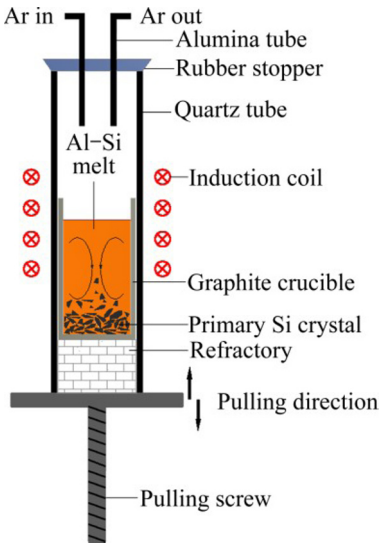

Fig. 1 Schematic diagram of experimental setup

3 Results and discussion

3.1 Enrichment of primary silicon

Figure 2 shows the cross-sections of the enriched samples, which reveal that the Si crystals agglomerated mostly in the lower part of the samples. The separation phenomenon could be attributed to the combined effect of electromagnetic stirring and the axial temperature gradient. Figure 3 shows a simulation diagram of the Si enrichment mechanism. During the enrichment process, a mushy zone formed between the melt and the enrichment zone owing to the axial temperature gradient,

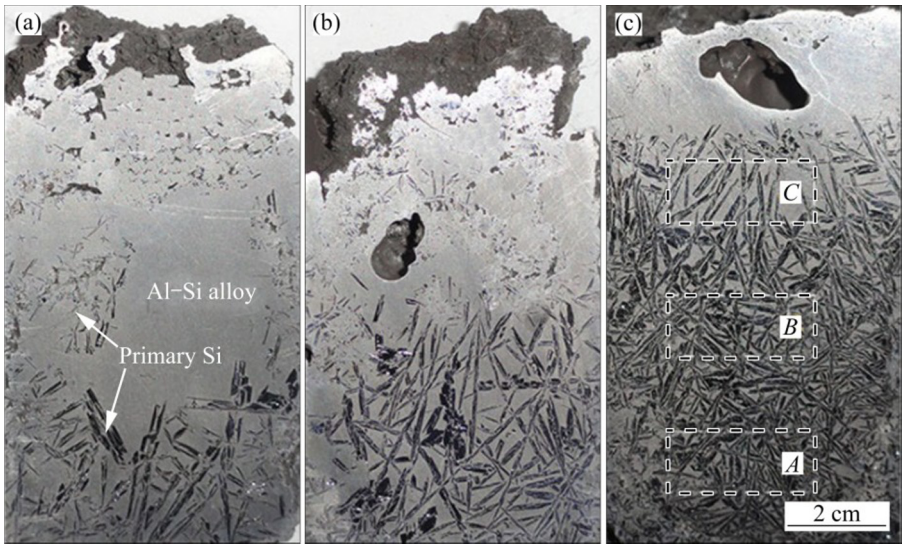

Fig. 2 Cross-sections of enriched samples: (a) Al−25%Si; (b) Al−35% Si; (c) Al−45% Si

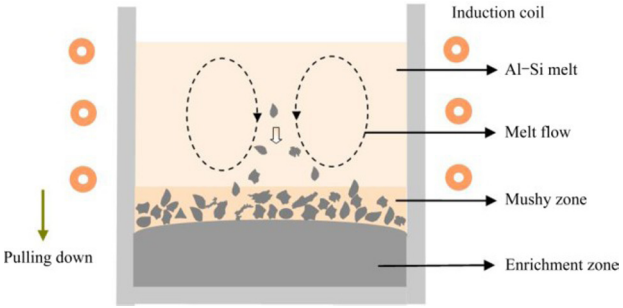

Fig. 3 Simulation diagram of Si enrichment mechanism

which was confirmed in our previous work [22,23]. As the temperature decreased to the liquidus line, the Si crystals began to nucleate and grow, and they were then pushed to the mushy zone owing to the electromagnetic stirring. The temperature of the mushy zone should be lower than that of the melt and the viscosity of the mushy zone should be higher than that of the melt; the Si crystals can easily adhere to the mushy zone when they approach it. Gradually, the mushy zone was entrapped by the solid/liquid interface to become the enrichment zone and a new mushy zone formed again near the enrichment zone.

From the enrichment zones depicted in Figs. 2(a)−(c), it can also be seen that the Si crystal content increased as the initial Si content increased; this indicates that a higher Si content could result in more efficient enrichment of Si crystals. Under the condition of steady-state diffusion, the growth velocity of Si crystals is mainly dependent on Si content in the melt; a higher Si content in the melt should of course raise the growth driven force and thus promote the Si crystal content. However, considering that electromagnetic stirring was performed during solidification, the steady-state diffusion could be disrupted to some extent. Hence, the impacts of melt stirring and melt viscosity on the Si crystal distribution should be taken into account. For example, numerous Si crystals are present outside the enrichment zone, as seen in Figs. 2(a) and (b), which indicates that the melt viscosity of the mushy zone may be a key factor influencing the enrichment of the Si crystals. If the viscosity of the mushy zone is not high enough, the Si crystals will also be pulled back to the melt from the mushy zone by the electromagnetic stirring.

It is necessary to emphasize that the viscosity of the mushy zone is related to the temperature, solid volume fraction, or, perhaps, the magnetic field. Temperature may be the most important factor for changing the viscosity of the mushy zone in accordance with the well-known Arrhenius equation, given in Eq. (1):

$$\eta = \eta_0 \exp\left(\frac{E_a}{RT}\right) \tag{1}$$

where η is the viscosity of the melt, E_a is the activation energy for viscous flow, η_0 is the pre-exponential viscosity, T is the temperature, and R is the mole gas constant. However, the axial temperature gradient of each sample remains constant during the enrichment process, which can result in the impact of temperature on the experimental results being ignored. The magnetic field may be another factor affecting the viscosity of the mushy zone, as expressed in Eq. (2) [24]:

$$\eta=\eta_0+kB^2 \tag{2}$$

where k is a ratio coefficient related to the electrical conductivity of the melt and the radius of the Si grain and B is the intensity of the magnetic field. It is worth emphasizing that the magnetic field induced by the alternating current is very low (in the range of $(0.01−0.04)T$ in this experiment). This may still result in

the impact of the magnetic field on the viscosity of the mushy zone being ignored. The relation between the viscosity and the solid volume fraction can be simply established by adopting Einstein's original results [25], as given in Eq. (3).

$$\eta=\eta_0(1+2.5f_S) \quad (3)$$

where f_S denotes the solid volume fraction of the melt. It has been shown that the viscosity is proportional to the solid volume fraction.

Figure 4 shows the relationship between the solid volume fraction and the alloy composition at different temperatures. The data for calculation were derived from the Al−Si binary diagram [26]. It is clearly seen that the solid volume fraction increased with increasing Si content of the Al−Si alloy at the same temperature.

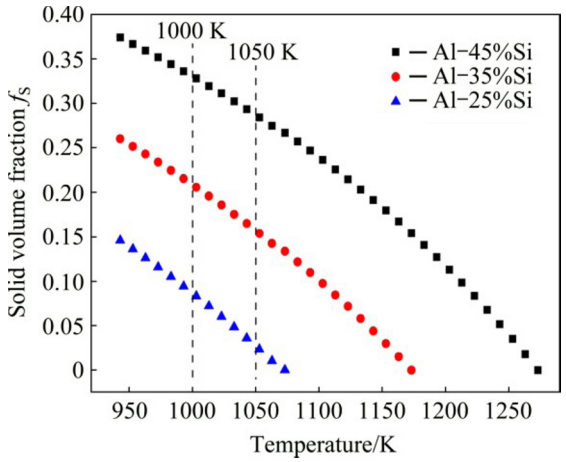

Fig. 4 Solid volume fraction dependence of temperature

Figure 5 shows the measurement results of the melt viscosity. The numerals in parentheses are the solid volume fractions. The melt viscosity was found to increase sharply with increasing solid volume fraction. Through fitting of the discrete data in Fig. 5, we can obtain values of η_0 and E_a by transforming Eq. (1) to the logarithmic Eq. (4).

$$\ln\eta=\ln\eta_0+\frac{E_a}{RT} \quad (4)$$

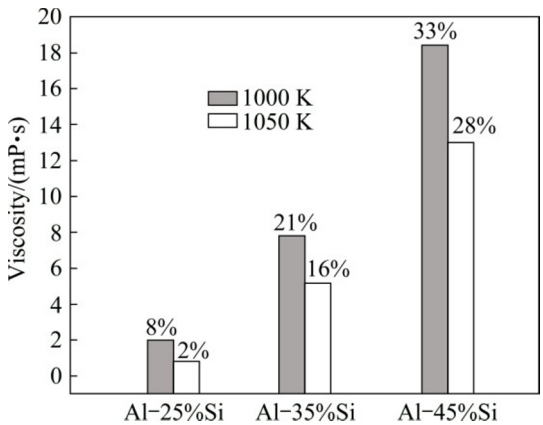

Fig. 5 Measurement results of viscosity

An Arrhenius plot, as shown in Fig. 6, can be obtained from Eq. (4). The calculated data of η_0 and E_a are listed in Table 1. It should be noted that E_a can be regarded as the temperature sensitivity of the viscosity. Obviously, the viscosity of Al−25%Si plays a more important role in temperature sensitivity than those of Al−35%Si and Al−45%Si. This implies that the viscosity is affected mainly by the solid volume fraction when the solid volume fraction is high. Conversely, when the solid volume fraction is low, the viscosity is affected mainly by temperature. These results suggest that the solid volume fraction is the most important factor governing the viscosity of the mushy zone in this experiment. However, SONG et al [27] have also reported values of E_a in the case of an Al−12%Si eutectic alloy, which are much smaller than those determined in the present work. This significant difference can possibly be attributed to the difference in liquid structures between the eutectic alloy and the hypereutectic alloy.

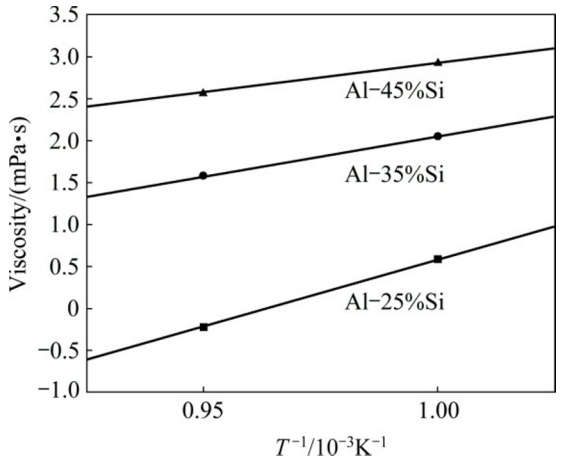

Fig. 6 Arrhenius plot of experimental data (scattered points) and fitting lines

Table 1 Calculated values of η_0 and E_a

Alloy	η_0/(mPa·s)	E_a/(J·mol^{-1})	T/K
Al−12%Si [27]	0.2356	9316.4853	843
Al−25%Si	0.904×10^{-7}	141595.734	1000−1050
Al−35% Si	0.448×10^{-3}	81186.210	1000−1050
Al−45% Si	0.0109	61806.276	1000−1050

Based on these experimental results, the adhesion ability of the mushy zone in Al−45%Si must be better than those in Al−35%Si and Al−25%Si, which will result in higher Si crystal content. However, other factors affecting the Si crystal content cannot be ignored. For example, with the progress of enrichment, the solid volume fraction of Al−45%Si will decrease to that of Al−35%Si, which will result in the same Si crystal content in these alloys. However, in reality, the Si crystal contents in most regions of Al−45%Si (shown in

Fig. 2(c)) are higher than those of Al−35%Si (shown in Fig. 2(b)). The reason for this result is the difference in the numbers of Si nuclei in these alloys. Obviously, there are more Si nuclei in Al−45%Si than in Al−35% because of the higher Si content in the former. After the Si nuclei are pushed to the mushy zone adjacent to the bottom of the sample, subsequent crystal growth will occur continuously. Thus, the Si crystal concentration can also be dependent on the number of initial Si nuclei.

Figure 7 shows the quantitative Si contents in regions *A* to *C* shown in Fig. 2(c). It can be seen that the contents of Si in regions *A*, *B*, and *C* are 65%, 55%, and 30%, respectively. Obviously, the enrichment efficiency of primary silicon decreases from the bottom to the top of the sample. This implies that the adhesion ability of the mushy zone varies during the enrichment process. It is necessary to emphasize here that the solid volume fraction of the melt must decrease gradually since the Si crystals are enriched continuously, which, in turn, will weaken the viscosity of the mushy zone with the progress of the enrichment. Therefore, control of the melt viscosity in the mushy zone is important for achieving high-efficiency enrichment.

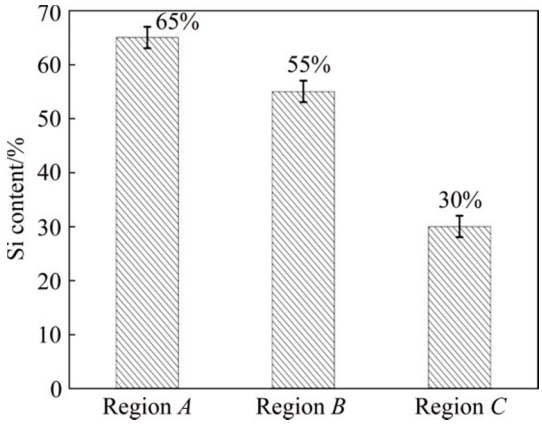

Fig. 7 Si contents in different regions of Al−45%Si sample

Figure 8(a) shows an enhanced process of enrichment of Si crystals. To maintain a constant solid volume fraction in the Al−Si melt, metallurgical-grade Si powder was continuously added to the melt during the enrichment process. The experimental result is shown in Fig. 8(b); a highly uniform Si crystal content is found in most regions of the enrichment zone, as can be observed at position I in Fig. 8(b). The upper part of the enrichment zone shows a sharp decline in the Si crystal content owing to the termination of the feed in the final stage, as observed at position II in Fig. 8(b).

The above-described analysis proves that higher-viscosity melt would be beneficial for the adhesion of Si crystals. However, it needs to be emphasized that high viscosity will have an adverse effect on the transportation of Si crystals to the enrichment zone. Therefore, the intensity of electromagnetic stirring should be a key factor for overcoming the problem of Si crystal transportation as well as achieving efficient enrichment of primary silicon. The relationship between Si crystal transportation and electromagnetic stirring has been discussed in our previous work [23].

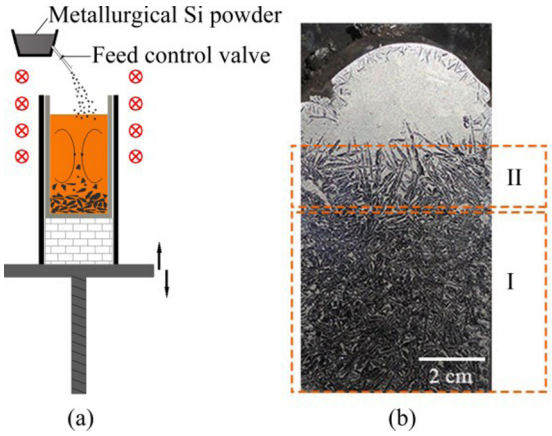

Fig. 8 Schematic of enhanced process of enrichment (a) and cross-section of sample enriched by enhanced process (b)

3.2 Morphology of primary silicon crystals

Figure 9 shows the micro morphologies at positions I and II in Fig. 8(b). It can be seen that the morphology of enriched Si crystals changes from spheroidal to plate-like in shape. It should be noted that several factors may affect the morphology of Si crystals. Of these, the dominant influencing factor is the Si content in the Al−Si melt. Additionally, the melt viscosity is expected to be another important influencing factor, since the diffusion of Si atoms in the melt can be strongly dependent on this factor.

Figure 10 shows the XRD analysis results of the Si-enriched crystals at positions I and II indicated in Fig. 8(b). Obviously, the preferential growth face of Si crystals at position II is (111). Further, the preferential growth plane of Si crystals at position I is (311). It is well known that the close-packed plane of Si crystal is the (111) plane, which can usually form a plate-like morphology. The transportation of Si atoms has been considered to be the most dominant parameter for the formation of plate-like Si crystals [28]. Therefore, the morphology of Si crystals can be easily affected by the melt viscosity, since it is an important factor governing the transportation of Si atoms. On the other hand, the enrichment zone can also be regarded as a porous medium, because the irregular shape of Si crystals causes this zone to become porous. According to Darcy's law [29], the movement of fluid in a porous medium has some relationship with the porosity structure. Thus, to eliminate the residual melt from the enrichment zone and improve the enrichment efficiency, it is important to

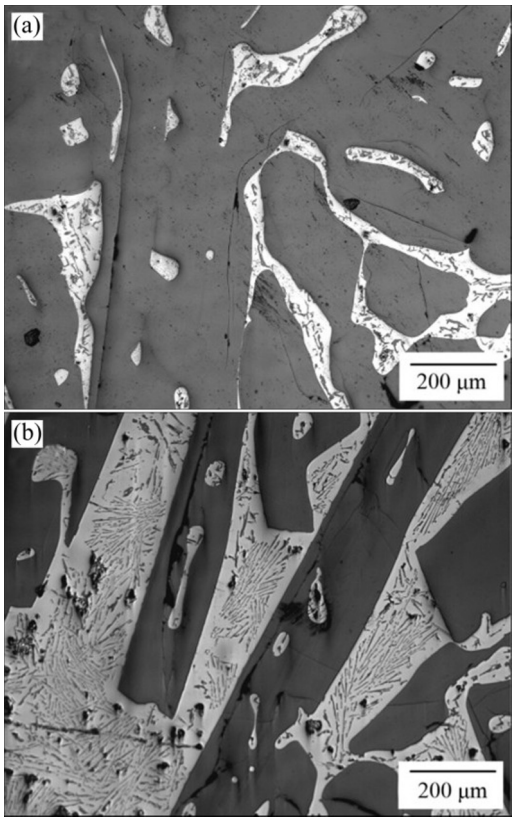

Fig. 9 Microstructures at position I (a) and position II (b)

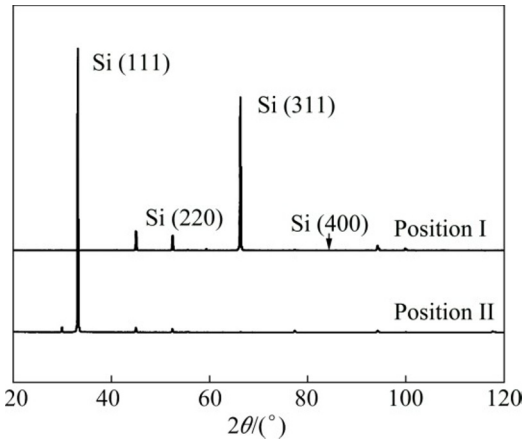

Fig. 10 XRD pattern analysis of Si-enriched crystals

control the morphology of Si crystals in the enrichment zone.

3.3 Separation of primary Si from Al−Si melt

Figure 11 shows the schematic diagram of the Si separation process. After the Si crystals in the lower part of the sample have been enriched, the Al−Si melt in the upper part can be poured out to achieve separation of Si. It should be noted that the Al−Si melt viscosity is the most important factor governing the pouring process, as well. A very high melt viscosity may increase the difficulty of pouring. Therefore, control of the viscosity of Al–Si melt to appropriate values will result in perfect separation of Si from the melt.

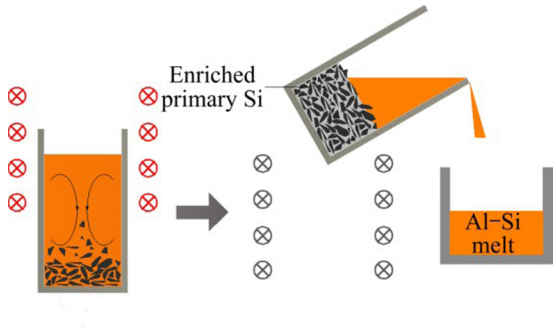

Fig. 11 Schematic diagram of Si separation process

Figure 12 shows the results of the separation experiment. Here, it is necessary to clarify that the pulling distances in Figs. 12(a)−(c) are 6 cm, 8 cm, and 10 cm, respectively. Further, it should be noted that Si crystals are gradually enriched to the lower part of the sample during the pulling-down process. Thus, the pulling distance is the key factor in deciding whether or not the enrichment is complete. In Fig. 12(a), it is seen that the Si crystals have not been completely enriched in the lower part of the sample, which results in a high Si content and high viscosity of the upper Al−Si melt. Therefore, pouring of the upper Al−Si melt from the sample is difficult owing to the poor mobility of the melt. In Fig. 12(b), it is seen that most of the upper Al−Si melt has been poured out from the sample; the poured Al−Si melt is shown in Fig. 12(d). As shown in Fig. 12(c), almost all of the upper Al−Si melt has been poured out from the sample; in this case, the poured Al−Si melt exhibits excellent mobility, as shown in Fig. 12(e). The microstructures of the poured alloy in Figs. 12(d) and (e) are shown in Fig. 13.

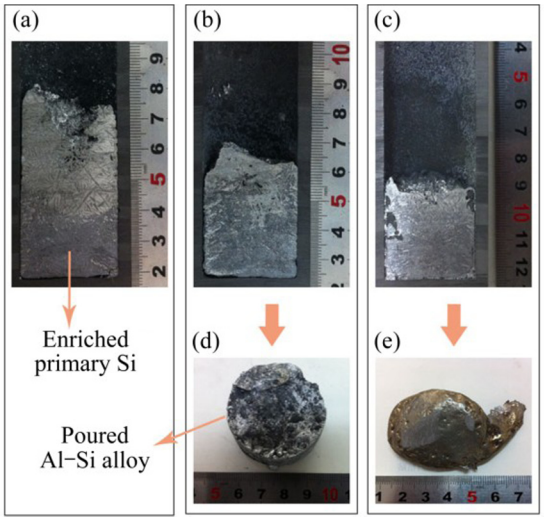

Fig. 12 Cross-sections of samples with different pulling distances: (a) 6 cm; (b) 8 cm; (c) 10 cm; (d, e) Poured Al−Si alloy after separation process

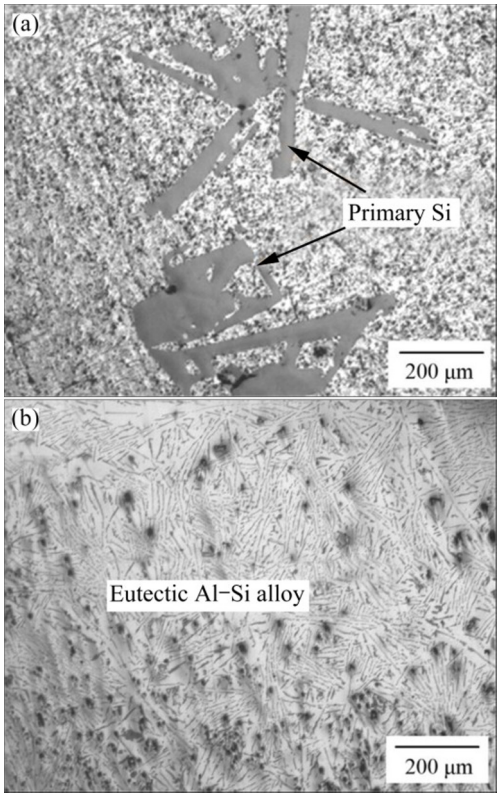

Fig. 13 Microstructures of poured Al−Si alloy for pulling distance of 8 cm (a) and 10 cm (b)

A considerable amount of Si crystals are observed to remain in the poured alloy when the pulling distance is 8 cm, as shown in Fig. 13(a). On the contrary, the poured alloy exhibits a eutectic structure when the pulling distance is 10 cm, as shown in Fig. 13(b). Obviously, the solid volume fraction in the former case is larger than that in the latter case, which results in the melt viscosity in the former case being higher than that in the latter case. These results simultaneously prove that the mobility of the melt can be affected by its viscosity, which is the determining factor for the separation process. This leads to the conclusion that the melt viscosity not only plays an important role in the enrichment of Si crystals but also affects the separation process. These results are expected to be useful in the development of a continuous or semi-continuous process for Si separation from the Al−Si melt, which will further reduce the manufacturing cost of high-purity Si.

4 Conclusions

1) The melt viscosity plays an important role in the enrichment of primary silicon in Al−Si melt. A higher viscosity of the mushy zone is beneficial to the adhesion of primary silicon crystals which will promote the efficiency of enrichment.

2) An improved enrichment process has been proposed to obtain a high-efficiency enrichment of primary silicon by controlling the melt viscosity constant.

3) The morphology of Si crystals changed from spheroidal to plate-like in shape in different regions of enrichment zone owing to the different viscosities.

4) The separation of enriched Si crystals and Al−Si melt was found to be dependent on the viscosity of the melt. A lower viscosity facilitated the separation due to the better mobility of this melt.

References

[1] MA Xiao-dong, YOSHIKAKA T, MORITA K. Phase relations and thermodynamic property of boron in the silicon-tin melt at 1673 K [J]. Journal of Alloys and Compounds, 2012, 529: 12−16.

[2] DIETL J. Hydrometallurgical purification of metallurgical-grade silicon [J]. Solar Cells, 1983, 10(2): 145−154.

[3] WU Ji-jun, MA Wen-hui, LI Yan-long, YANG Bin, LIU Da-chun, DAI Yong-nian. Thermodynamic behavior and morphology of impurities in metallurgical grade silicon in process of O_2 blowing [J]. Transactions of Nonferrous Metals Society of China, 2013, 23(1): 260−265.

[4] WEI Kui-xian, MA Wen-hui, YANG Bin, LIU Da-chun, DAI Yong-nian, MORITA K. Study on volatilization rate of silicon in multicrystalline silicon preparation from metallurgical grade silicon [J]. Vacuum, 2011, 85(7): 749−754.

[5] WU Ji-jun, LI Yan-long, MA Wen-hui, WEI Kui-xian, YANG Bin, DAI Yong-nian. Boron removal in purifying metallurgical grade silicon by CaO−SiO_2 slag refining [J]. Transactions of Nonferrous Metals Society of China, 2014, 24(4): 1231−1236.

[6] GAN Chuan-hai, FAN Ming, ZHANG Lei, QIU Shi, LI Jin-tang, JIANG Da-chuan, WEN Shu-tao, TAN Yi, LUO Xue-tao. Redistribution of iron during directional solidification of metallurgical-grade silicon at low growth rate [J]. Transactions of Nonferrous Metals Society of China, 2016, 26(3): 859−864.

[7] MARTORANO M A, FERREIRA NETO J B, OLIVEIRA T S, TSUBAKI T O. Refining of metallurgical silicon by directional solidification [J]. Materials Science and Engineering B, 2011, 176(3): 217−226.

[8] HANAZAWA K, YUGE N, KATO Y. Evaporation of phosphorus in molten silicon by an electron beam irradiation method [J]. Materials Transactions, 2004, 45: 844−849.

[9] YOSHIKAWA T, MORITA K. Refining of silicon during its solidification from a Si−Al melt [J]. Journal of Crystal Growth, 2009, 311(3): 776−779.

[10] HU Lei, WANG Zhi, GONG Xu-zhong, GUO Zhan-cheng, ZHANG Hu. Purification of metallurgical-grade silicon by Sn−Si refining system with calcium addition [J]. Separation and Purification Technology, 2013, 118: 699−703.

[11] MITRAŠINOVIĆ A M, UTIGARD T A. Refining silicon for solar cell application by copper alloying [J]. Silicon, 2009, 1(4): 239−248.

[12] KHAJAVI L, MORITA K, YOSHIKAWA T, BARATI M. Removal of boron from silicon by solvent refining using ferrosilicon alloys [J]. Metallurgical and Materials Transactions B, 2015, 46(2): 615−620.

[13] GU Xin, YU Xue-gong, YANG De-ren. Low-cost solar grade silicon purification process with Al-Si system using a powder metallurgy technique [J]. Separation and Purification Technology, 2011, 77(1): 33−39.

[14] KIM K Y, JEON J B, SHIN J S. Centrifugal separation of primary silicon crystal in solvent refining of silicon using Al−30% Si alloy [J]. Crystal Research and Technology, 2014, 49(10): 761−767.

[15] LI Ya-qiong, TAN Yi, LI Jia-yan, MORITA K. Si purify control and separation from Si−Al alloy melt with Zn addition [J]. Journal of Alloys and Compounds, 2014, 611: 267−272.
[16] BAN Bo-yuan, BAI Xiao-long, LI Jing-wei, CHEN Jian, DAI Song-yuan. Effect of kinetics on P removal by Al−Si solvent refining at low solidification temperature [J]. Journal of Alloys and Compounds, 2016, 685: 604−609.
[17] YU Wen-zhou, MA Wen-hui, LV Guo-qiang, REN Yong-sheng, XUE Hai-yang, DAI Yong-nian. Si purification by enrichment of primary Si in Al−Si melt [J]. Transactions of Nonferrous Metals Society of China 2013, 23(11): 3476−3481.
[18] YOSHIKAWA T, MORITA K. Refining of Si by the solidification of Si−Al melt with electromagnetic force [J]. ISIJ International, 2005, 45: 967−971.
[19] LI Xi, REN Zhong-ming, FAUTRELLE Y. Effect of a high gradient magnetic field on the distribution of the solute Si and the morphology of the primary Si phase [J]. Materials Letters, 2009, 63(15): 1235−1238.
[20] HE Yan-jie, LI Qiu-lin, LIU Wei. Effect of combined magnetic field on the eliminating inclusions from liquid aluminum alloy [J]. Materials Letters, 2011, 65(8): 1226−1228.
[21] JIE J C, ZOU Q C, SUN J L, LU Y P, WANG T M, LI T J. Separation mechanism of the primary Si phase from the hypereutectic Al−Si alloy using a rotating magnetic field during solidification [J]. Acta Materialia, 2014, 72: 57−66.
[22] YU Wen-zhou, MA Wen-hui, LV Guo-qiang, XUE Hai-yang, LI Shao-yuan, DAI Yong-nian. Effect of electromagnetic stirring on the enrichment of primary silicon from Al-Si melt [J]. Journal of Crystal Growth, 2014, 405: 23−28.
[23] XUE Hai-yang, LV Guo-qiang, MA Wen-hui, CHEN Dao-tong, YU Jie. Separation mechanism of primary silicon from hypereutectic Al−Si melts under alternating electromagnetic fields [J]. Metallurgical and Materials Transactions A, 2015, 46(7): 2922−2932.
[24] JIN Fang-wei, REN Zhong-ming, REN Wei-li, DENG Kang, ZHONG Yun-bo, YU Jian-bo. Effects of a high-gradient magnetic field on the migratory behavior of primary crystal silicon in hypereutectic Al−Si alloy [J]. Science and Technology of Advanced Materials, 2008, 9: 1−6.
[25] EINSTEIN A. A new determination of the molecular dimensions [J]. Annalen der Physik, 1906, 19: 289−306.
[26] MURRAY J L, MCALISTER A J. The Al−Si (aluminum−silicon) system [J]. Bulletin of Alloy Phase Diagrams, 1984, 5(1): 74−84.
[27] SONG Xi-gui, BIAN Xiu-fang, ZHANG Jing-xiang, ZHANG Jie. Temperature-dependent viscosities of eutectic Al−Si alloys modified with Sr and P [J]. Journal of Alloys and Compounds, 2009, 479: 670−673.
[28] XU C L, JIANG Q C. Morphologies of primary silicon in hypereutectic Al−Si alloys with melt overheating temperature and cooling rate [J]. Materials Science and Engineering A, 2006, 437(2): 451−455.
[29] CHEVALIER T, CHEVALIER C, CLAIN X, DUPLA J C, CANOU J, RODTS S, COUSSOT P. Darcy's law for yield stress fluid flowing through a porous medium [J]. Journal of Non-Newtonian Fluid Mechanics, 2013, 195: 57−66.

铝硅熔体黏度对初晶硅富集和分离的影响机制

余文轴[1]，马文会[2]，郑 忠[1]，蒋伟燕[1]，李 杰[1]，田茂洪[1]

1. 重庆大学 材料科学与工程学院，重庆 400044；
2. 昆明理工大学 冶金与能源工程学院，昆明 650093

摘 要：研究了铝硅合金电磁分离过程中熔体黏度对初晶硅富集和分离的影响。结果表明，熔体黏度对初晶硅的富集效率和分离有决定性的作用。高黏度熔体有利于初晶硅的富集，反之低黏度熔体可以促进初晶硅的分离。基于此，对初晶硅富集过程的机理进行了新的解释，并通过控制熔体黏度获得了一种强化初晶硅富集效率的工艺。此外，熔体不同区域黏度的差异会导致初晶硅的晶体形貌由球状转变为板片状。

关键词：定向凝固；电磁搅拌；铝硅熔体；初晶硅；分离；黏度

(Edited by Yun-bin HE)